Stochastic Longshore Current Dynamics

Juan M. Restrepo[a,1], Shankar Venkataramani[b]

[a] *Department of Mathematics, and College of Earth, Ocean, and Atmospheric Sciences, Oregon State University, Corvallis, OR 97331, USA*

[b] *Department of Mathematics and Program in Applied Mathematics, University of Arizona, Tucson AZ 85721, USA*

Abstract

We develop a stochastic parametrization, based on a 'simple' deterministic model for the dynamics of steady longshore currents, that produces ensembles that are statistically consistent with field observations of these currents. Unlike deterministic models, stochastic parameterization incorporates randomness and hence can only match the observations in a statistical sense. Unlike statistical emulators, in which the model is tuned to the statistical structure of the observation, stochastic parametrization are not directly tuned to match the statistics of the observations. Rather, stochastic parameterization combines deterministic, i.e physics based models with stochastic models for the "missing physics" to create hybrid models, that are stochastic, but yet can be used for making predictions, especially in the context of data assimilation.

We introduce a novel measure of the utility of stochastic models of complex processes, that we call *consistency of sensitivity*. A model with poor consistency of sensitivity requires a great deal of tuning of parameters and has a very narrow range of realistic parameters leading to outcomes consistent with a reasonable spectrum of physical outcomes. We apply this metric to our stochastic parametrization and show that, the loss of certainty inherent in model due to its stochastic nature is offset by the model's resulting consistency of sensitivity. In particular, the stochastic model still retains the forward sensitivity of the deterministic model and hence respects important structural/physical constraints, yet has a broader range of parameters capable of producing outcomes consistent with the field data used in evaluating the model. This leads to an expanded range of model applicability. We show, in the context of data assimilation, the stochastic parametrization of longshore currents achieves good results in capturing the statistics of observation *that were not used* in tuning the model.

Keywords: longshore currents, stochastic parametrization, parameter sensitivity, consistently of model sensitivity, data assimilation.

1. Introduction

Longshore (alongshore) currents are ubiquitous oceanic flows in nearshore environments (see [1], for a descriptive review). The two mechanisms responsible for their existence are wave stresses and alongshore sea elevation gradients. Because longshore currents affect nearshore bathymetry and beach morphology, and are responsible for a great deal of nearshore transport, models for these currents are of great practical utility.

Presently, deterministic wave-resolving models are used with good results, capturing some of the complex dynamics of the nearshore, including longshore currents (see [2], [3], [4], [5]. See also [6]). Of note are wave-resolving, depth-integrated models based upon the Boussinesq equations, such as funwaveC ([7]). These have shown considerable forecasting skill (See for example, [8], and [9], in which field data on eddy variability and dye and drifter dispersion are compared to funwaveC model output). The success of funwaveC in capturing a wide range of nearshore oceanic phenomena rests upon its generality: it includes higher

*Corresponding author

Email address: restrepo@math.oregonstate.edu (Juan M. Restrepo)

order dispersion (see [10]), a general bottom drag parametrization (see [8]), wave breaking momentum transformation parametrization via Newtonian damping (see [11]) and the breaking viscosity model [12].

Non-wave resolving complex models of the nearshore ocean environment exist as well. These also have compared favorably with certain aspects of longshore current dynamics and observations, such as longshore shear instabilities. They can also capture other nearshore flows, such as rip currents, consistent with observations ([13], [14], [15] and references contained therein).

None of the models capture longshore current observations in a statistically faithful manner. By fidelity we mean that the time series generated by the model and the observations are indistinguishable, statistically. The most familiar modeling approach to improving model fidelity is to resolve and include more physics (or better physics). The present state-of-the-art in longshore modeling is the wave-resolving models mentioned above. An approach that directly focuses on obtaining statistical fidelity is statistical emulation (see [16]). In this strategy observations are used to build phenomenological models. The fundamental modeling strategy consists of proposing a basic statistical distribution or a regression model. Structure is built into the model by calibrating the model's correlations and other statistical dependences with data.

The goal of this paper is to propose and demonstrate the use of an alternative modeling approach, called stochastic parametrization. It is an intermediate between the deterministic and the emulator approaches to modeling physical phenomena. This strategy yields a model that has as much structure and physics as possible, leaving as little as possible to chance. A good stochastic parametrization yields structure in the statistics of its time series by the blend of deterministic and stochastic elements, rather than by tuning the model using data to incorporate the correlations and structure of the observations.

A common use for stochastic parametrization is to incorporate in a computationally efficient way unresolved dynamics that cannot be ignored even if the model focused on large spatio-temporal scale phenomena. A familiar practical example of deterministically parametrizing small scales is via homogeneization (see [17]): when the small scales offer a certain amount of scale separation and it is statistically homogeneous, the small scale averages that persist appear in the resulting deterministic model as complementary or added terms. A more sophisticated approach, in computational fluid mechanics, is large eddy simulations (LES) of turbulent flows. In that case the complementary/added terms themselves have their own dynamics which come from closures of higher moment statistics. Stochastic parametrization is meant to increase a model's fidelity, but unlike LES, it will not do so rationally. For the longshore current model featured in this paper the stochastic parametrization will be used to capture the small scale variability present in the observations, enhancing this way its fidelity, not its rationality.

In this study we will purposely choose the simplest possible model for longshore current dynamics, a balance model, as a starting point. Clearly, a model that already has improved physics would be a better choice for the development of an operational stochastic model, but a simple and familiar model makes it plain, to what extent the stochastic parametrization is effective in enhancing the original deterministic model's fidelity. Balance models for longshore currents capture nothing more than the most basic of physical processes, albeit under strong assumptions. Nearly all of the physics in longshore current models are captured by empirical parametrization: the models incorporate parametrized wave radiation (or the vortex force), wave breaking, turbulence, stress and drag forces. The longshore model we will use is derived from the vortex force formulation for the evolution of waves and currents in the nearshore (see [18], and [19]). The vortex force model is a general, non-wave resolving, model. It was used in [20] to describe the evolution of rip currents, as well as longshore currents in [15]. This model (see Appendix A) will be referred to as the *vortex force model*, in order to distinguish it from the simpler and specialized *balance model* for longshore current dynamics.

The plan of the rest this paper is as follows: after describing essential background to the nature of the data, in Section 2, we introduce in Section 3 the longshore balance model that will be used as a basis for the stochastic parametrization. Section 3 discusses the conditions under which the longshore balance model is derived from the non wave-resolving, wave-current interaction, vortex force model. Stochastic parametrization can lead to better *consistency of model sensitivity*, at the expense of increased uncertainty. The topic of consistency of sensitivity will be taken up in Section 4. A model that has consistent sensitivity will have a wide range of physically-meaningful parameter combinations with which to capture a broad spectrum of physical outcomes. The balance model will be used to explore and illustrate the consequences of

sensitive consistency. The stochastic parametrization, inspired by the data and constrained by the physics of longshore currents, is introduced in Section 5. Stochastic parametrization of unresolved physics, as evidenced by the data, is used to construct a stochastic balance longshore model. Suggesting a simple model for observational data that is clearly non-Gaussian will lead us to introduce Gaussian mixtures. With this choice of stochastic parametrization the stochastic longshore model is shown to compare favorably with observations. Notably, the model captures correlations present in the data without having to explicitly put these into the model. Furthermore, the stochastic longshore model will be shown to have consistent sensitivity. However, the use of Gaussian mixtures reduces the fidelity of the model. The point of using the mixture model will nevertheless make the model amenable to simple linear/Gaussian data assimilation methods. Data assimilation is a very useful methodology for combining observations and models. Stochastic models are well suited for this application, as will be shown in Section 6, using the proposed stochastic longshore model and observations in a concrete data assimilation example calculation.

2. Longshore Current Observational Data

In the process of constructing a stochastic parametrization, as well as in testing the resulting stochastic model, we will make use of field observations. We will use the data set collected in Duck, North Carolina by Herbers, Elgar, Guza, and Birkemeier, Long and Hathaway (see [21]). Henceforth, we shall refer to this data as the *Duck data*. The Duck data repository provides data, and in particular, information on nearshore flow mean velocity. It also has recordings of ocean pressure, temperature, and depth, over the course of several months. It also contains information on the peak frequency, direction, and sea elevation amplitude of incoming waves. Bathymetry as well as the conditions under which the data was obtained is available as well. The Duck data as well as ancillary information are available from:
`frf.usace.army.mil/pub/Experiments/DUCK94/SPUV`.

A plot of a typical bottom topography cross section appears recreated in Figure 1. The plot also shows the data collection devices and data collection locations. The cross shore and longshore components of the velocity were collected at a sampling rate of 2 Hz for 10784 seconds, every 3 hours. The data collection spanned the months of August, September, October, and early November, 1994. Sporadic instrumentation failure lead to interruptions in data collection. The cross-shore velocity component is zero on average for most of the data gathering campaign, and is ignored in this study. The specific "SPUV data" streams we will make use of are from measurement locations v12, v13, v14, v15, which were located approximately at the offshore coordinates 205, 220, 240, and 260m, respectively. The transect we will work with is at roughly 930m in the alongshore (y) direction. At these stations the data exhibits good signal to noise characteristics. The locations correspond a location right before the waves shoal and break. We will also be using another set of data, collected during the same time period as the SPUV longshore current data, and it consists of wave elevation, wave period, and wave direction, further out from shore, roughly 900 m offshore, where the water depth is approximately 8m. This data is available from `frf.usace.army.mil/pub/Experiments/DUCK94/FRF`. Figure 2 shows a more general view of the bathymetry, reconstructed from October 1994 data. As can be seen, the alongshore variability in the bathymetry is mild and is used to justify picking a single y-location for the data. In any event, our focus is on the methodology of stochastic parametrization, rather than on observations or the validity of the specific model chosen.

3. The Longshore Current Balance Model

One of the earliest balance models for longshore currents is due to Longuet-Higgins [22, 23]. In his model longshore currents are driven by the wave radiation stress (see [24, 25]). Several several simplifying assumptions were made in the formulation of the model: the current was assumed steady, the bottom $h(x)$ was assumed to be gently sloping, *i.e.*, with a slope $\beta := dh/dx$, where x is the (offshore) distance from the shore, in the range $0 < \beta \ll 1$. The bottom was also assumed featureless, and void of alongshore y dependence. Nonlinear effects were ignored, wave refraction was ignored and the angle of incidence of the

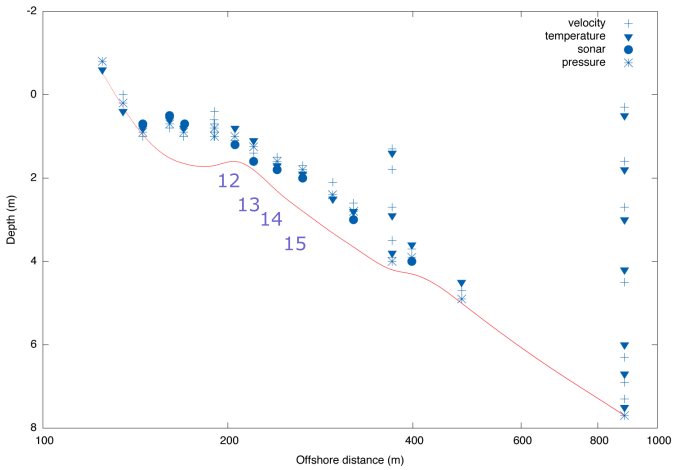

Figure 1: Cross section of bathymetry, along the transect $y = 929.8$m. The type of measurements that were collected are indicated. Stations v12-v15 are indicated as well.

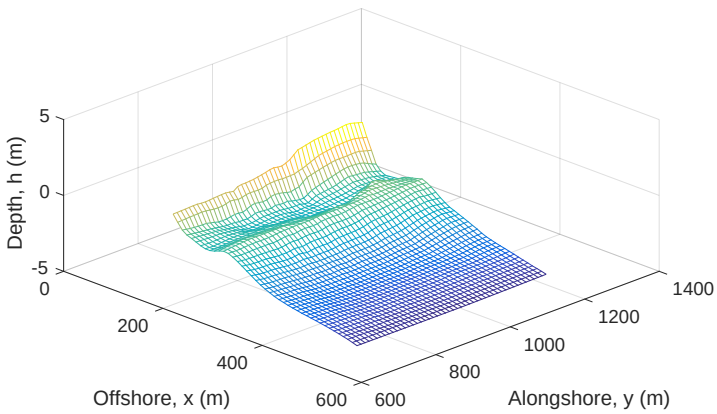

Figure 2: The bathymetry, October 1994. The Duck bathymetry is characterized by mild changes in the topography in the alongshore direction, compared to changes in the crossshore direction.

waves was assumed to not differ considerably from the normal to the beach. Finally, the water column depth H was approximated by the depth h, which is the distance from the bottom to the quiescent sea level.

In its classic form the model suggests that longshore currents result from a balance of the drag force $\mathbf{D}$, the gradient of the (transverse) radiation stress tensor S due to waves, and dissipation $\mathbf{N}$. With the depth-averaged and time-averaged current denoted by $\mathbf{u} = (u, v)$, the current v is given by the y-component (alongshore) of the momentum balance. The balance reads

$$0 = -c_D\, v - \frac{\partial S_{xy}}{\partial x} + N \frac{\partial}{\partial x}\left(\sqrt{gh}h\frac{\partial v}{\partial x}\right). \tag{1}$$

The first term on the right hand side on (1) is the bottom drag, with a particularly simple parametrization: the drag force is proportional to the current, $c_D \geq 0$ is the proportionality constant. The second term is the gradient of the net stress per unit area due to waves, where $S_{xy} \approx \sigma W \cos\theta \sin\theta$. W is the wave action, σ is the wave frequency. The angle θ is with respect to the coordinate x, normal to the shore. The last term is the y-component of the lateral dissipation, N is a dimensionless tunable parameter. This particular dissipation model was suggested by Longuet-Higgins, [22, 23]. It is based upon dimensional arguments and makes many approximations including the assumption that the longshore currents occur over mildly sloped bathymetry. (See [26], for an analysis and discussion of this dissipation model and some of its alternatives).

In what follows we will use a similar and equally simple balance model. We will denote it the *Longshore Balance Model*, hereon. The model derives from the *Vortex Force* model for wave current interactions, which is described in Appendix A. Similar assumptions as those made by Longuet-Higgins take us from the vortex force model to the longshore balance model (see discussion leading to (A.11). The longshore model is

$$0 = -c_D\, v + \alpha \frac{\beta_B}{h^5} + N \frac{\partial}{\partial x}\left(\sqrt{gh}h\frac{\partial v}{\partial x}\right). \tag{2}$$

In (2)

$$\alpha := 12/\sqrt{\pi} g B_r^3/\gamma^4 \geq 0, \qquad \beta_B := A^7 k \sin(\theta).$$

The wavenumber magnitude is k. the sea elevation is A, and g is gravity. B_r and γ are parameters associated with wave breaking and sea elevation, respectively.

The longshore balance model is equivalent to a balance model proposed by Thornton and Guza [27]. When they compared their model to field data, obtained off the gently sloping coast of their test site in California (USA), they found good agreement. This agreement seemed not to depend in any strong way on having dissipation. However, when they compared their model to data obtained over a barred beach, such as the Duck site data, their model was inadequate. Further analyses of comparisons of models and the Duck data associated with the DELILAH field campaign [28] brought into question the linear model for the bottom drag force, and further, the need for a spatially varying bottom friction in order to get better agreement between model and data. Over the years several improved models for the bottom drag have been proposed. See, for example, [29], for a bottom drag model that is directly inspired by the Duck and SuperDuck data sets. Nevertheless, we will keep the linear bottom drag model in the longshore balance model, since it leads to special modeling challenges and the goal of this work is to demonstrate stochastic parametrization as a tool with which to improve model fidelity.

4. Consistency of Sensitivity Analysis

There are several practical reasons for an analysis of the model's sensitivity, to either forcing/boundary conditions, initial conditions, or parameters. One reason is to identify which of these has the most impact (usually in the linearized sense) on the model outcomes (see [30]). Sensitivity and uncertainty are two different things, but they are sometimes intertwined. Another reason is to diagnose sensitive dependence on initial conditions in evolution equations. Sensitive dependence is a hallmark of chaotic systems. Yet another reason is to evaluate the robustness of numerical approximations to evolution equations.

The most common way to assess these sensitivities is by a forward linearized approach. In forward sensitivity analysis we want to determine how relative perturbations of the outputs depend on relative perturbations of the inputs (in backward sensitivity analysis we instead ask what relative inputs are required to produce a certain relative perturbation of the output).

In similar fashion, one could also determine explicitly or implicitly the functional relationship between model outcomes and perturbations of parameters. One outcome is to determine whether a broad spectrum of physical outcomes are reached by reasonable and sensible range of parameters. How large should one determine the ranges of outputs and input parameters? One reasonable approach is to seek similar ranges in the physics of its measurements and the physical variables that inform the parameters in the model. Consistency of sensitivity (to parameters) is similarity in the structure and the relative magnitudes of variations in the model outcomes to variations in the parameters, and their measured values. Clearly, the concept is qualitative and it is not universally applicable: some model parameters have no physical counterpart.

Forward (linear) sensitivity analysis is used to determine the explicit dependency of longshore velocity fluctuations on the wave forcing. These fluctuations are with respect to the ensemble mean, denoted by $\langle\cdot\rangle$. In what follows we will ignore the lateral dissipation, as it is thought to be less critical to longshore dynamics than the other forces in the longshore balance model (see [28]). Ignoring dissipation in (2) we get the balance equation

$$\frac{c_D}{h}\langle v\rangle = \alpha\frac{\langle k\sin\theta A^7\rangle}{h^6}, \tag{3}$$

The sensitivity of the longshore current is obtained by taking the first variation to obtain

$$\frac{c_D}{h}\langle\Delta v\rangle + \frac{\Delta c_D}{h}\langle v\rangle \approx \left(\frac{\Delta k}{k} + \frac{7\Delta A}{A^7} + \frac{\cos\theta\Delta\theta}{\sin\theta}\right)\langle v\rangle. \tag{4}$$

The sensitivity in the angle, even when small, can be physically dramatic when the average angle of incidence is nearly zero since $\sin(\theta)$ in the denominator is small. Nevertheless, we will focus in this study on the variability of velocity fluctuations to changes in A and c_D. Concerning these,

$$\langle\Delta v\rangle \propto \frac{k\sin\theta A^7}{h^5 c_D}\left(\frac{7\Delta A}{A} - \frac{\Delta c_D}{c_D}\right).$$

We denote the wave amplitude supplied by wave forcing from the deep waters as A_∞. Since $A = A(A_\infty)$ (see ahead, in (8), for the specifics), we approximate ΔA by ΔA_∞, and assume that the relative variability in the amplitude $\Delta A/A \gg \Delta c_D/C_D$, the relative variability in the drage coefficient. With these approximations,

$$\langle\Delta v\rangle \approx \text{const}\frac{k\sin\theta}{h^5}\frac{\Delta A_\infty}{c_D}. \tag{5}$$

We refer to (5) as the drag-wave forcing *sensitivity analysis estimate*, and we will build a stochastic parametrization that respects, to a certain extent, this analysis.

4.1. Consistency of sensitivity analysis for the Deterministic Model

There are two challenges in using data to tune model parameters. Posed as questions, what sort of statistics do we apply on the data to affect the comparison to the model? And the more challenging question, for a given set of parameters, do we retain consistency with the inherent structure of the model, for a reasonable range of model inputs?

The Duck data will be used to tune the model represented by (2). (The dissipation will be ignored). The entire 8m depth offshore time series data set for k, θ, and A_∞ is used to get estimates of their mean values. (The dispersion relationship (A.1) and wave number conservation (A.2) equations are required to relate the observed wave period to k). The wave action equation (A.4) is needed to relate A at the measuring stations to the observational data, A_∞, obtained in the deeper waters. We then proceed by finding c_D so that the mean data for v at station v13 coincides with the predicted value of v, via (2), at that location.

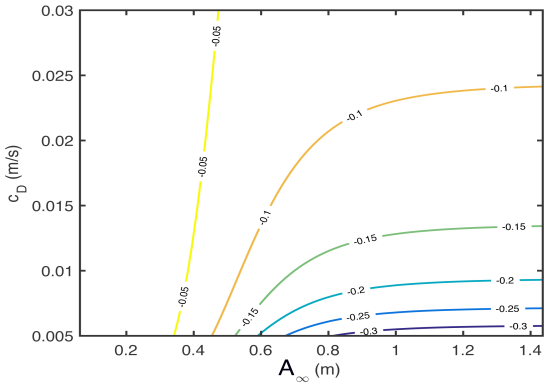

Figure 3: Sensitivity curves for the balance model, (2), in (A_∞, c_D) parameter space. The model was forced using observational data captured in 8m depth offshore waters. For the wave forcing a a time average value is used. Time average values were also used for θ and for k. The contours represent the mean of the difference between the estimated velocity and the measured velocity at station v13.

Figure 3 shows contours of discrepancy between the value of the calculated and observed longshore velocity at station v13. We note that for small off shore wave amplitudes A_∞, the longshore velocity is relatively insensitive to the drag parameter, while for large A_∞, the longshore velocity is indeed sensitively dependent on c_D. The conclusion from this exercise is that for certain data one is forced to choose unphysical combinations of (A_∞, c_D) to obtain agreement between model outcomes and field data, or parameter choices that make the model unacceptably sensitive. Both of these issues are symptomatic of inconsistency of the sensitivity: even if one obtains reasonable agreement between the model and the data some of the combinations that lead to agreement between model and data may not respect the sensitivity estimate, (5). (Fortunately the situation is less dramatic when the (full) complex model is used instead and is tuned to obtain reasonable agreement with data).

The model we chose is simply too crude and thus the inconsistency is extreme, reflecting the fact that the model is missing some of the important physics of the problem, and the simple physical mechanisms that are retained in the model are incapable of describing the observations with reasonable values for the model parameters. It is not hard to see that such inconsistency of sensitivity is also shared by the more complex vortex force model. However, stochasticity can be introduced to tame the inconsistency, as will be shown in what follows.

5. A Stochastic Balance Model for Longshore Currents

The goal is to produce a simple, consistent in sensitivity, balance model for longshore currents. This will be accomplished by enhancing a balance model via stochastic parametrization in order to account for the short-time variability observed in the data. The short-time variability cannot be captured by the original balance model (2), even when the forcing is obtained from the 8m water observations. Clearly, a great deal of physics is missing. We will only pursue stochastic parametrization rather than to complement the crude model with better or more physics.

We will begin with an analysis of the data. Two data sets will be used in the model formulation. The "8m offshore" wave data largely informs β_B in (2), and a longshore time series data will be used as "training data." We will then compare the training data, which is the longshore velocity time series at a specific location, to the longshore model driven by the 8m wave data. The parameter c_D in the drag force will be calibrated to enhance the role played by the drag term in (2) in constributing to the empirical histogram that results from a comparison of the training data and the longshore model driven by the 8m offshore data. The remaining discrepancies in the empirical distributions are then brought to a minimum by the addition of a stochastic parametrization of momentum contributions. The discrepancy in the histograms of the forcing and the longshore velocity is presumed largely due to missing physics in the original balance

Table 1: *First row: empirical statistics of the time series V, the longshore velocity v (m/s) at station v13. Subsequent rows: the wave quantities, measured at 8m depth offshore location: the period T in seconds, the significant wave height H_{mo}, and wave direction θ (degrees). Duck data, September, 1994.*

variable	mean	median	mode	standard deviation
V (m/s)	0.0373	-0.0130	-0.032	0.2931
$T = 2\pi/\sigma$ (s)	9.907	9.706	13.56	3.114
$H_{mo} = 2\sqrt{2}A_\infty$ (m)	0.8272	0.6410	0.3850	0.5821
θ (degrees)	-2.160	-4.000	-8.000	21.15

model. A model that assigns to stochasticity as little of the model fidelity as possible is preferred, and further, we favor simple noise processes rather than complicated ones. We will use make frequent use of Gaussian mixtures to capture non-Gaussianity. See [31] for details on Gaussian mixtures.

5.1. Analysis of the Data

We will be focusing on longshore velocity field data from one particular location, station v13. This is the "training data." We will denote this data time series as V, in what follows. Some of the basic statistics on the V data appear in Table 1. These statistics pose a challenge to the balance model (2) and it is apparent in Figure 3: if we use mean values for the data A_∞ as well as $k(T)$ and θ and we insist that the drag force parameter c_D is positive, the model will generate a negative mean estimate for V. One might think that using the more complex model presented in the Appendix will circumvent the conundrum, however, the derivation of the longshore balance mode using the vortex force model as a starting point makes it plain that the problem would be present had the vortex force model be used. (One could use the median or modal values for the quantities in question, but the model appearing in the Appendix is a mean-field model (see [32, 18])).

We use instead an ensemble modeling approach. The wave forcing will be computed via (8) using the 8m depth offshore wave forcing data. Before constructing the stochastic longshore model we will examine aspects of the statistics of the data that provide valuable physical constraints for the modeling process. We begin, however, with finding approximations to the empirical probability distribution functions (pdfs) of the data. Figure 4 shows that a Gaussian mixture [33] approximates well the pdfs of the sea elevation, wave direction, and wave frequency of the 8m depth offshore data. We specifically use the Expectation-Minimization Algorithm (EM, hereon) in the Gaussian mixture calculations. Superimposed, and appearing as dashed lines, are the 2 Gaussians used in the pdf mixture representation. We highlight the skewness of the distributions. Skewness is also evident in the Gaussian mixture approximation of the empirical histogram of V. See Figure 5a. In Figure 5b we display the time series of the longshore velocity V, for several months, starting on August 1 and running till the end of October, 1994. This data was used to produce the empirical histogram for V. Prominent in the time series is the faster variability occurring at the hourly time scale, as well as the slower variability changing on multi-day time scales.

The connection between the offshore data and the longshore velocity is through the term

$$\beta_B(A_\infty, k, \theta, x) = A^7(x; A_\infty)k(x; \sigma)\sin(\theta). \tag{6}$$

The β_B appears in the second term on the right hand side of (A.11) and in the second term on the right hand side of (2) (see also (A.9)). The term $\alpha\beta_B/h^6$ is a parametrization of momentum exchanges between wave breaking processes and currents. The relationship between k, the wavenumber and the 8m offshore frequency data is found via the dispersion relation (A.1). The relationship between the amplitude $A(x)$ and the 8m offshore wave amplitude data is found approximately as follows: assuming that the variability of the waves is not resolvable at the current time scales, (A.4) is then

$$\frac{d}{dx}[W\mathbf{C}_g] = -\frac{\epsilon}{\sigma}, \tag{7}$$

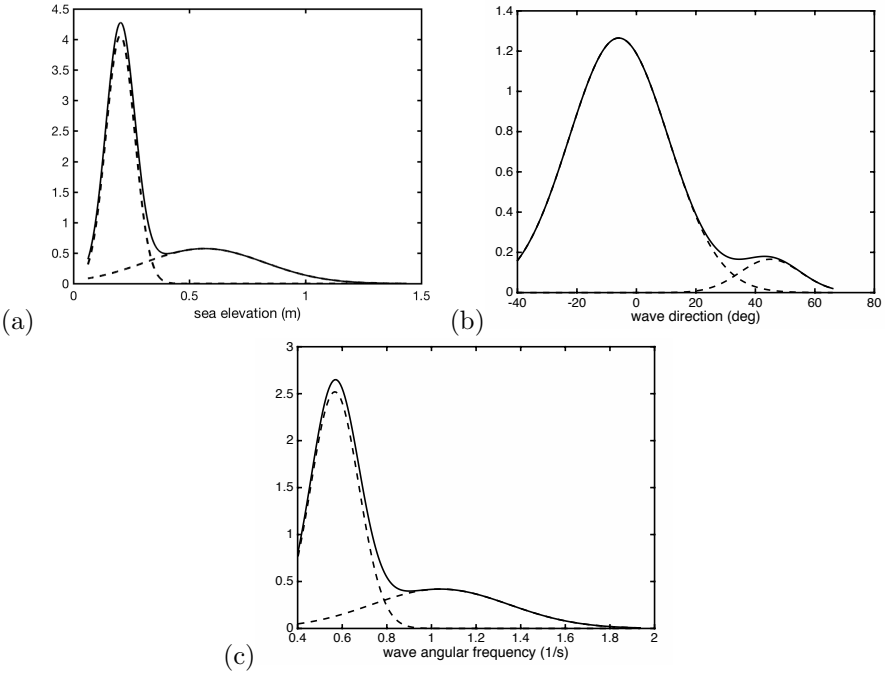

Figure 4: Duck wave data (8m depth offshore data). Histograms of the (a) sea elevation (wave height) (m), (b) wave direction (degrees) and (c) angular frequency (1/s). The times series was collected at a 2 Hz rate, continuously for 8192 seconds, every 3 hours, during August-October, 1994. Gaussian mixture, solid, the two Gaussians of the mixture, dashed.

ignoring alongshore variation and taking $H \sim h$, and the group velocity $|\mathbf{C}_G| \approx \sqrt{gh}$ (the group velocity is otherwise found to be given by (A.5)). The dissipation term ϵ is defined in (A.9). The wave amplitude is then given approximately, by

$$A(h; A_\infty) = h^{-1/4}[h_\infty^{-5/4} A_\infty^{-5} - \tilde{\delta}(h^{-23/4} - h_\infty^{-23/4})]^{-1/5}, \tag{8}$$

with $\tilde{\delta} = \frac{10\delta}{23\beta}$. See [34]. Here, $\delta = 2\alpha\sigma g^{-3/2}$. The amplitude of the waves, or wave forcing, is A_∞, at depth $h_\infty := \beta x_\infty$. The depth $h_\infty \approx \lambda/20$, where λ is the wave wavelength. This is a depth at which there is less than a 1% discrepancy between H and h in the shallow water wave limit, kH (we note that (8) can yield unphysical results, as it can lead to A being zero for certain values of h). The model for ϵ (see A.9) could be modified to account for viscous dissipation, which becomes more prominent very near to the shore. (In [35] it is shown that stochastic variability meant to capture episodic wave breaking leads to a Stokes drift velocity that has the familiar deterministic component as well as a diffusion-dominated term, however, this type of dissipation would be overwhelmed by nearshore breaking).

In the stochastic parametrization approach we work with ensembles. We first need to create a distribution for β_B. Samples of β_B can be produced via rejection Monte Carlo sampling (see [36]), using the 8m offshore data. The empirical historgram that results from the rejection sampling using the offshore data appears in Figure 6. This distribution was obtained under the assumption that the samples from A, k and θ were independent. We note that the distribution obtained this way is skewed and very narrow (it is even narrower and similarly skewed when the assumption of independence is not used).

As we will discuss presently, a comparison of the empirical autocorrelation times of the 8m offshore data and the training set V will play a critical role in assessing the resulting stochastic longshore balance model. Figure 7a portrays the autocorrelation τ_β of time-ordered β_B, which found using the 8m depth offshore wave data as input. The correlation time τ_β is about a day. It is comparable to the autocorrelation time τ_V, which corresponds to the longshore current time series data at location v13 (see Figure 7b). There are 3 important points to make in connection with the results portrayed in Figure 7: the autocorrelation length

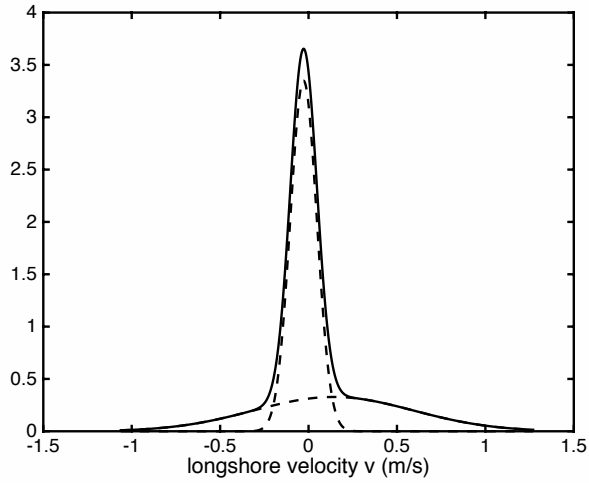

(a)

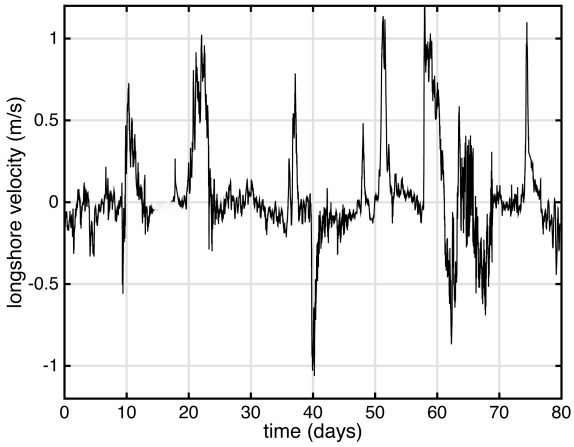

(b)

Figure 5: Duck data. Longshore velocity V. Time series data at station v13 (measured about 220m offshore), starting on August 1, 1994. (No data is available during days 14-17). The empirical, Gaussian mixture appears in (a) as dashed curves. Superimposed is the empirical pdf of the longshore velocity V. The distribution is non-Gaussian, *i.e.*, skewed. The time series of V appears in (b).

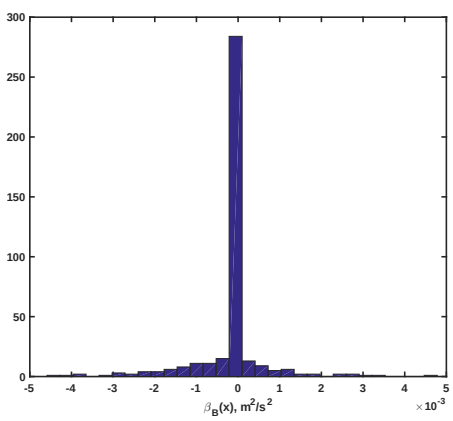

Figure 6: Histogram of β_B. See (6). Computed by drawing samples of k, A, and θ, assuming these are independent. Note skewness.

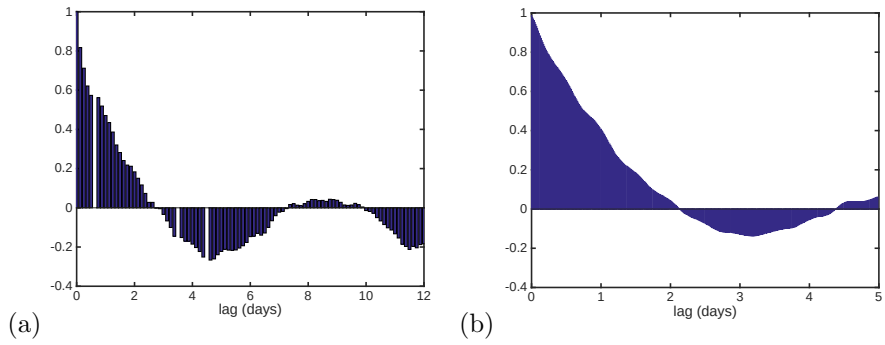

Figure 7: (a) The autocorrelation τ_β of β_B, using $A(A_\infty), k, \theta$ observations as input. We denote this the autocorrelation time τ_β and it is about 1 day. It is found by calculating a time series of β_B from time-ordered triplets of $A(A_\infty), k, \theta$ observations. In (b) we display the autocorrelation τ_V. This is the autocorrelation of the time series of the longshore velocity data at station v13. We note that τ_β is comparable to τ_V.

is similar in the stochastic model and in the data; the autocorrelation length is mainly set by the wave forcing; the stochastic model rightly delivers the autocorrelation; it was not tuned or manipulated to agree with data.

5.2. Formulating an Uncertainty Model via Stochastic Parametrization

There are 4 terms in the momentum balance, (A.11). As we noted in the previous section, the variability of empirical distributions of V and of the term $\alpha\beta_B/h^6$ are very disparate. The bottom drag coefficient c_D is tuned to obtain a certain balance with the term $\alpha\beta_B/h^6$. We will use tune c_D so that the support of the empirical distribution of $c_D V$ and $\alpha\beta_B/h^5$ are comparable. The estimate for $c_D \approx 0.007$ m/s.

The time series for V is suggestive of at least two time scales in the dynamics. The drag term $c_D v$ and the momentum exchange $\alpha\beta_B/h^5$ term, are meant to dominate the momentum balance at the longer time scales. The computed time autocorrelations shown in Figure 7 in fact support the claim that there are two very disparate time scales, $h/c_D \ll \tau_\beta$. These disparate time scales provide reasonable justification to lump all of the short-time missing physics, collectively represented by $\partial v/\partial t$, by an additive stochastic term. In [4, 5] this short term variability is ascribed to shearing instabilities (see [13]). Shorter time scale wave breaking is also noted as a significant fast-time influence on longshore currents (see [6]). We thus proceed with the stochastic parametrization, focusing on capturing the missing fast-time variability.

First, since the mean of the data-informed $\alpha\beta_B/h^6$ and of $c_D V/h$ are not the same, the balance of these two terms will on average be non-zero, leading to a steady acceleration and thus a bias in the longshore current. In view of these constraints we propose a stochastic model for the predicted velocity $v(x,t) := \langle V\rangle + v_0(x) + v'(x,t)$, where $\langle V\rangle$ is the data mean. The space-time solution of $v_0(x)$ appears in Figure 8. The *stochastic longshore velocity balance model* we propose (which for completeness includes the lateral dissipation) reads

$$0 = (\mathcal{L} - \frac{c_D}{h})v_0 - \alpha\frac{\langle\beta_B\rangle}{h^6} + \alpha\frac{\beta_B}{h^6} - \frac{c_D}{h}v'(x,t,\eta_t), \tag{9}$$

$$v'(x,t,\eta_t) = \sum_{\ell=1}^{N_\ell} f_\ell(x,t)P_\ell(\eta_t). \tag{10}$$

$\mathcal{L}w = N\frac{1}{h}\frac{\partial}{\partial x}\left(\sqrt{gh}h\frac{\partial w}{\partial x}\right)$. η_t is a random variable with known associated distribution $\rho(\eta_t)$. P_ℓ are (in this instance) Hermite polynomials of degree $0 \le \ell \le N_\ell$. The expansion coefficients f_ℓ are found via standard projection, since $\int_{-\infty}^{\infty} P_\ell(\eta_t)P_j(\eta_t)\rho(\eta_t)d\eta_t = \sqrt{\pi}\delta_{\ell,j}$. The Gaussian measure $\rho(\eta_t)$ is obtained from observational data. The Gaussianity of this measure is assumed and it represents measurement "error." See [37] for further details.

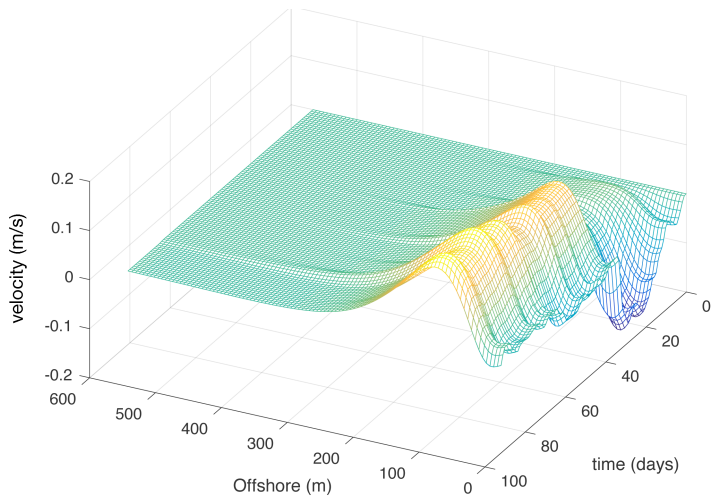

Figure 8: Space-time plot of $v_0(x)$.

Since the model in question is simple we will dispense with the polynomial chaos representation in favor for a crude Gaussian mixture parametrization of v'. Specifically,

$$v'(t) = \sum_{\ell=1}^{N_\ell} a_\ell \mathcal{N}_t(m_\ell, \sigma_\ell(v_0)), \tag{11}$$

$\mathcal{N}_t$ are Gaussian variates. v' can have a non-zero mean. The input to the EM is the data-informed quantity $-c_D(V - \langle V \rangle) + \alpha/(\beta_B - \langle \beta_B \rangle)/h^5$, at x corresponding to station v13. For the data under consideration $N_\ell = 2$ was adequate. An empirical histogram of v' is shown in Figure 9. Using dashed lines we highlight the 2 Gaussians in the mixture. In what follows we will assign $\ell = 1$ in (11) to the narrow Gaussian in the mixture, and label the broader one by $\ell = 2$. The Gaussian mixture captures the empirical pdf well, and the model is complete.

In the next section we will apply the model in a data assimilation exercise. Stochastic models are well suited to Bayesian inference since they can provide concrete priors. In anticipation of this application, we will actually suggest a less accurate but considerably simpler representation for v'. It is clear that the mixture component centered at the mode, the $\ell = 1$, has very narrow variance and could be approximated by its mode. We retain the $\ell = 2$ Gaussian mixture component. The stochastic longshore balance model, simplified, is thus

$$v(x,t) \approx -\frac{\alpha}{c_D}\left[\mathcal{L} - \frac{c_D}{h}\right]^{-1} \frac{\beta_B(x)}{h^6(x)} - a_1 + a_2 \mathcal{N}_t(m_2, \sigma_2). \tag{12}$$

where $a_1 = 0.04$, $a_2 = 0.4$, $m_2 = 0.04$, $\sigma_2 = 0.4$. Adjusting for means, Figure 10 superimposes $v(x)$ at station v13, given by (12), and V.

6. Data Assimilation using the Stochastic Balance Model

We apply the stochastic longshore balance model in a data assimilation setting of longshore current data. (See [38], for background on data assimilation, with an emphasis on geophysical applications). Since the model (12) is linear and Gaussian, an optimal estimator is found via least-squares, or sequentially, via Kalman filtering. We opt for the Kalman filter. The Kalman estimator minimizes the trace of the posterior, time dependent conditional probability distribution of the longshore velocity. The Kalman filter will deliver the time dependent ensemble mean and variance of the posterior distribution of the longshore velocity, given observations, taking into account model error and observational errors, both assumed known.

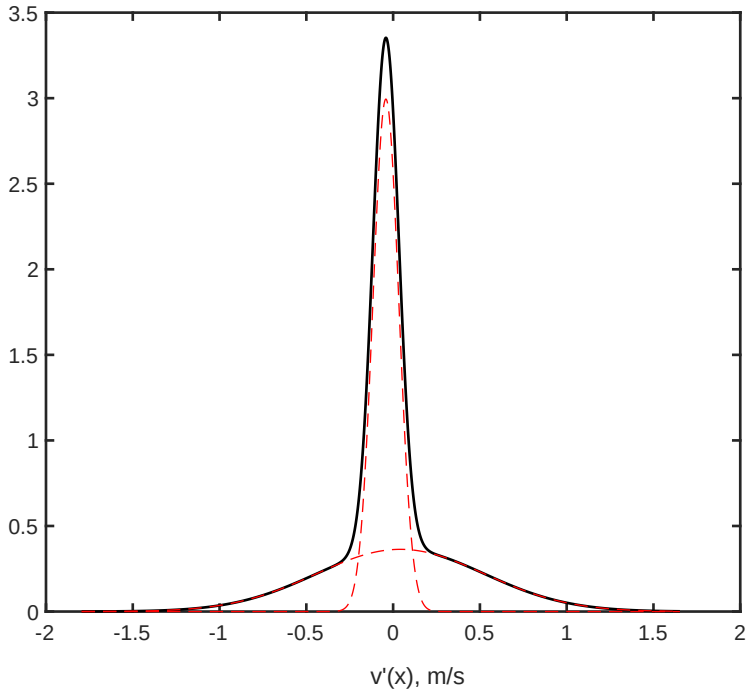

Figure 9: Empirical pdf for v' (see also Figure 5a).

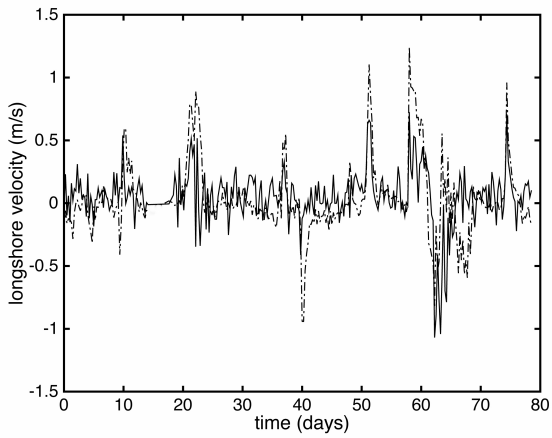

Figure 10: Time series of $V - \langle V \rangle$ (dashed) and model outcome $v(x,t) - \langle V \rangle$ at x corresponding to station v13 (solid).

To clarify what this simple illustrative calculation demonstrates, we mention the following: the *state variable* to be estimated is the time history of the longshore velocity at some location, given observations of the longshore velocity at that location. In order to make the problem more interesting we chose to estimate the longshore velocity at station v14, which is about 20m further offshore than location v13. Let V_{14} denote the velocity at station v14. The ingredients in this exercise are, (1) the actual data V_{14}, which is to be called *truth* and used to assess how good our estimate is; (2) the *model* which is a simple discretization of the stochastic longshore model, evaluated at station v14; (3) the *data*, which consists of noisy longshore data V_{14}, at regular time intervals. (The noise is meant to emulate measurement error. Obviously, the station data comes equipped with measurement errors, however, the inherent variability of the signal does not reflect the measurement error itself).

The goal is to show that the assimilation of data and the model produces a reasonable estimate of the ensemble mean and variance of the distribution of V_{14}. Note that the data V_{14} is highly non-Gaussian in its distribution and thus higher order moments are not going to agree. Moreover, this estimate should be better than that obtained by the model alone or the observations alone. The quality of the estimate is evaluated here by a simple comparison to the truth data, and expect that a good estimator is close to the truth. The model is stochastic, and as suggested in Figure 10, well trained to capture the data at v13. If we use the model only we will produce ensemble members that resemble those of Figure 10. At v14, the model yields a mean velocity estimate of $\langle v(\text{v14})\rangle = 0.0345$ m/s. The mean of the truth is $\langle V_{14}\rangle = 0.0311$ m/s. The model does reasonably well. If we were to use the data only to estimate truth, it will largely depend on how often we measure it and how large the measurement uncertainty is. Next we consider the data assimilated estimate.

Let ϕ_n be an approximation of the longshore data at time t_n. The discrete model for the longshore current and the relationship between the model variable ϕ_n and the observations $\{y_m\}_{m=1}^{M}$, respectively,

$$\begin{aligned} \phi_{n+1} &= p\phi_n + \Delta t q_n + B\Delta W_n, \quad n = 0,1,2..., \quad \text{the model,} \\ \phi_m &= y_m + C\Delta W_m, \quad m = 1,2,..,M, \quad \text{the data.} \end{aligned}$$

The discrete model is obtained by using the simplest possible discretization of (12). Here, $p = 1 - \Delta t c_D/h$, and $q_n = \Delta t \alpha k \sin\theta A^7/h^6$. We take $\phi_0 = -a_1 + a_2 m_2$, and $B = a_2\sigma$. The dissipation term will be omitted. In what follows we will be assuming that the discrete model times t_n and the data times t_m are commensurate. Also, we will assume that $\Delta t = t_{n+1} - t_n$ is constant for any n. Here ΔW_n and ΔW_m are uncorrelated normal increments with variances B and C, respectively, assumed time independent. C is set to $0.1B$. The Kalman filter formulas are

$$\begin{aligned} \hat{\phi} &= p\hat{\phi}_n + \Delta t q_n, \quad n = 0,1,2,... \\ \hat{u} &= p\hat{u}_n p + B_n, \quad n = 0,1,2,... \\ K_n &= \hat{u}(\hat{u} + C_n)^{-1}, \quad n = 0,1,2,... \\ \hat{\phi}_{n+1} &= \hat{\phi} + K_n(y_m - \hat{\phi})\delta_{m,n}, \quad m = 0,1,2,... \\ \hat{u}_{n+1} &= (1 - K_n)\hat{u}, \quad n = 0,1,2,.... \end{aligned} \tag{13}$$

where $\hat{\phi}_n$ and $\hat{u}_n$ are estimates of the mean and the uncertainty, respectively, of v_n. The "truth" is taken as the noise-free field data, which is a 60 day record of the longshore current at station v14, during September and October 1994. Figure 11 shows the truth, the estimate and the data, y_m, which is read every 5 time steps. The variance u_n of the posterior is estimated to be appproximately 0.035, which compares favorably with the (truth) data variance, estimated at 0.05. We conclude that the assimilated product stays close to the truth and further, that it is statistically consistent with it.

7. Summary

Parametrization usually refers to the application of empiricism rather than "first principles" in the formulation of some aspect or the totality of a model of some physical process. By first principles we mean

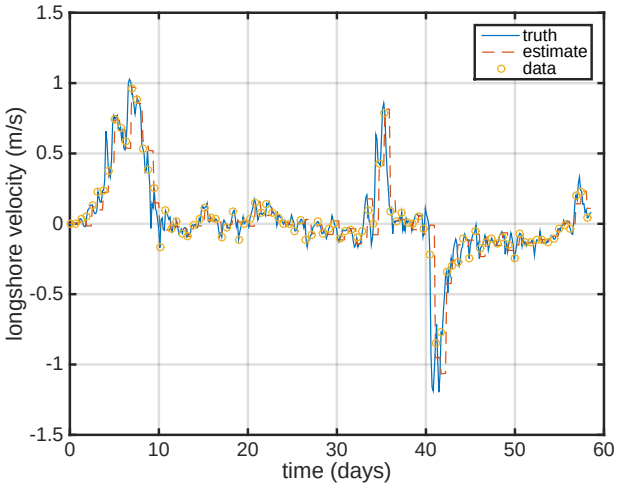

Figure 11: Estimation of the longshore velocity data (dashed) using a Kalman Filter and a simple discretization of the longshore model (12). The *truth* signal is field data (solid). The measurements (dots) are read every 5 time steps. The measurements has been synthetically perturbed by a normally-distributed process with variance 10 times greater than the variance inherent in the stochastic drag parameter.

fundamental laws of physics, or conservation or axiomatic principles (such as the least action principle). Parametrization is used a great deal in problems involving multi-physics and multi-scales and/or as a way to include an important phenomenon in a model that has not yielded to first principle explanations or that cannot be resolved. The forces in the longshore balance model are in fact empirically determined, even though it has a basis in conservation principles of mass, momentum, and energy. Stochastic parametrization produces a type of model that makes sense in the ensemble. The aspect that is parametrized in the model generally does not have a physical or rational basis, however, its inclusion in the model is critical to its fidelity. By fidelity we mean that it is consistent with data in an ensemble sense. Unlike stochastic emulators, which are also aiming for fidelity, and in which structure has to be derived from the data and explicitly added, a good stochastically parametrized model leaves to chance as little as possible and derives its structure from whatever physics is being captured by the model.

In this study we purposely picked a simple deterministic model to use to illustrate how one goes about the task of parametrizing missing physics via stochasticity. We could have instead used a more sophisticated model for longshore currents. For example one could start with (9)- (10), with (9) replaced by (A.8), or perhaps use a wave-resolving model such as funwaveC ([7])). The parametrization process would proceed in the same way. The simple longshore balance model, however, is simply understood and the role played by stochastic parametrization better understood and appreciated.

In our specific example the stochasticity was used to represent fast variability that was not resolved by the deterministic longshore balance model. A successful outcome of the parametrization is that the stochastic longshore model was able to display correlation times similar to those estimated from the data itself.

Situations when stochastic parametrization may be a viable modeling option abound. As we showed, one such situation is when unresolved but essential physics are important to the faithful representation of observations via models. Other situations introduce stochasticity into model parameters. One would like to ascribe as much of the phenomena being modeled to physically-based constructs, however, in some instances one is willing to exchange rationality for model robustness, or replace the notion of determinism for one in which ensembles make sense.

With regard to model robustness, stochastic parametrization may be a way to achieve better consistency of sensitivity. Models, particularly ones that have an overwhelming dependence on parametrization often have very delicate tuning of parameters and very limited ranges of physical relevance. Consistency of

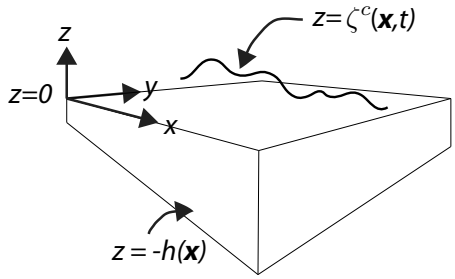

Figure A.12: Schematic of the nearshore environment, z increases above the quiescent level of the sea $z = 0$, $\mathbf{x} := (x, y)$, and t is the (long) time variable. The elevation component of the free surface associated with the currents is $z = \zeta^c(\mathbf{x}, t)$. The bottom topography $z = -h(\mathbf{x})$ is referenced to the quiescent sea level height, $z = 0$.

sensitivity is a property that allows one to assess whether the sensitivity of a model outcome to changes in parameters is similar to those found in the natural problem (in the event that the parameter is a physically-meaningful quantity). The consistency of sensitivity analysis could thus be used as a way to determine the parameter ranges expected for the expected spectrum of physical outcomes. A model that is consistent in sensitvity will be applicable to a wide variety of physical situations, using sensible or physically meaningful parameter combinations; conversely the analysis can also suggest when this is just not possible. Finally, consistency of sensitivity could be used to compare different models or as another tool for empirical analysis.

Practically speaking one can see how the introduction of stochasticity can make a model consistent in its sensitivity, at the expense of introducing uncertainty/randomness. Our claim is that it is sometimes a reasonable price to pay, especially in complex models of multi-scale/multi-physics phenomena. Furthermore, the introduction of stochasticity, provided it does not lead to a serious loss of rationality, can be exploited in a Bayesian setting, wherein forecasts are replaced by ensemble estimates and combine the stochasticity of the model itself and the uncertainties of observations via Bayesian inference and data assimilation.

Appendix A. The Vortex Force Wave Current Interaction Model

Non-wave resolving shallow-water models that capture longshore currents, forced by steady waves and no wind, have 2 known solution manifolds: steady longshore currents and unsteady ones (see [15] and references therein). The stability depends on the strength of the bottom drag, namely, when the drag acceleration is prominent, the longshore currents are steady. In what follows we assume that longshore currents are nearly steady and thus we require high drag values in the complex model to simulate these.

The depth-averaged, wave current interaction model in [18] is specialized to the nearshore environment. This is a model for the interaction of currents and waves at spatio-temporal scales much larger than those typical of the waves. A schematic of the domain, along with the coordinate system is described in Figure A.12. The transverse coordinates of the domain will be denoted by $\mathbf{x} := (x, y)$. The cross-shore coordinate is x and increases away from the beach. Time is denoted by $t \geq 0$. Differential operators depend only on $\mathbf{x}$ and t. The total water column depth is given by $H := h(\mathbf{x}) + \zeta^c(\mathbf{x}, t)$, where $\zeta^c = \hat{\zeta} + \zeta$, is the composite sea elevation. The sea elevation has been split into its dynamic component $\zeta(\mathbf{x}, t)$, and $\hat{\zeta}$, the quasi-steady sea elevation adjustment. $\hat{\zeta} = -A^2 k/(2\sinh(2kH))$, where A is the wave amplitude and k is the magnitude of the wavenumber $\mathbf{k}$. The wave frequency σ is given by the dispersion relationship

$$\sigma^2 = gk \tanh(kH), \tag{A.1}$$

where g is gravity, and the evolution of the wave number is found by the conservation equation

$$\frac{\partial \mathbf{k}}{\partial t} + \boldsymbol{\nabla}\omega = 0, \tag{A.2}$$

where $\omega = \mathbf{k} \cdot \mathbf{u} + \sigma$. $\mathbf{u}(\mathbf{x}, t) := (u, v)$ is the depth-averaged velocity (current) vector. The wave amplitude A is found by solving for the wave action

$$W := \frac{1}{2\sigma}\rho g A^2, \tag{A.3}$$

via the action equation,

$$\frac{\partial W}{\partial t} + \nabla \cdot (W\mathbf{c}_G) = -\frac{\epsilon}{\sigma}, \tag{A.4}$$

where ρ is the fluid density. The wave action dissipation rate is captured by $-\frac{\epsilon}{\sigma}$. The group velocity is $\mathbf{c}_G = \mathbf{u} + \mathbf{C}_G$, with $\mathbf{C}_G$ given by

$$\mathbf{C}_G = \frac{\sigma}{2k^2}\left(1 + \frac{2kH}{\sinh(2kH)}\right)\mathbf{k}. \tag{A.5}$$

The continuity equation is given by

$$\frac{\partial H}{\partial t} + \nabla \cdot [H(\mathbf{u} + \mathbf{u}^{\mathrm{st}})] = 0, \tag{A.6}$$

where

$$\mathbf{u}^{\mathrm{st}} := (u^{\mathrm{st}}, v^{\mathrm{st}}) = \frac{1}{\rho H} W\mathbf{k}, \tag{A.7}$$

is the Stokes drift velocity.

The velocity $\mathbf{u}$ is found via the momentum equation

$$\frac{\partial \mathbf{u}}{\partial t} + (\mathbf{u} \cdot \nabla)\mathbf{u} + g\nabla\zeta - \mathbf{J} = \mathbf{S} + \mathbf{N} + \mathbf{B} - \mathbf{D}. \tag{A.8}$$

The vortex force term (see [32]) is

$$\mathbf{J} = -\hat{\mathbf{z}} \times \mathbf{u}^{\mathrm{st}}\chi,$$

where χ is the vorticity, and $\hat{\mathbf{z}}$ is the unit vector pointing anti-parallel to gravity.

The terms on the right hand side of (A.8) model several physical processes critical to nearshore wave-current conditions, none of which have generally agreed-upon parametrizations: $\mathbf{S}$ and $\mathbf{N}$ represent the depth-averaged wind stress and sub-scale processes associated with viscous dissipation, respectively. Wave-to-current momentum exchanges due to the breaking waves are captured by

$$\mathbf{B} = \frac{\epsilon \mathbf{k}}{\rho H \sigma}.$$

There are several empirical formulations for ϵ (≥ 0). The one we adopt here is due to [27]. (See also [34]). It is

$$\epsilon = 24\sqrt{\pi}\rho g \frac{B_r^3}{\gamma^4 H^5}\frac{\sigma}{2\pi}A^7, \tag{A.9}$$

with B_r, γ, empirical parameters. This empirical relationship based upon hydraulic theory and has been fit and tested against data in nearshore environments similar to the nearshore case considered in this paper. The depth-averaged bottom drag is

$$\mathbf{D} = \frac{\boldsymbol{\tau}}{\rho H},$$

where

$$\boldsymbol{\tau} = \rho c_D \mathbf{u}, \tag{A.10}$$

where $c_D = c_f|\mathbf{u}_w| = \frac{2}{\pi}\tilde{c}_f|\mathbf{u}_w|$ is the *bottom drag* parameter. $|\mathbf{u}_w|$ is the wave orbital velocity, estimated near the bottom topography, and $\tilde{c}_f \geq 0$ the friction coefficient. In this particular bottom drag parametrization the friction coefficient $\tilde{c}_f$ (or the drag parameter c_D itself) needs to be calibrated/empirically determined. It is assumed that $|\mathbf{u}_w|$ is much larger that $|\mathbf{u}|$ (See [39], Chapter 5) and exhibits inherent variability at time scales of the waves, which are shorter the variability of the currents. This form of the bottom drag represents the most limited and simplest possible parametrization (we will purposely choose this parametrization for this exercise and stochastic parametrization, but other models could be used: The models of Soulsby [40, 41] and Feddersen and co-workers [29] are alternatives, the latter in fact has been tuned to conditions present in Duck NC. (See also [15] for a comparison of these different drag models).

Appendix A.1. The Longshore Current Balance Model

Similar assumptions are made in the derivation of this balance model as were made in connection with deriving (1). The longshore current v does not have y dependence. The wave-to-current momentum transfer due to wave breaking $\mathbf{B}$ is retained, as is the $\mathbf{N}$. Wind stresses are ignored, hence $\mathbf{S}$ is omitted. The crux of the derivation of a balance model for longshore currents, based upon the vortex force formulation of wave-currents, is the observation that the depth-averaged normal component of the velocity at the shore must be zero, and hence $u = -u^{St}$. Also for steady currents, the vortex force and the inertial terms balance, provided that the only contribution to the currents are wave-induced, *i.e.*, there are no remotely imposed currents or wind stresses to account for. The simple longshore momentum balance will be

$$\frac{\partial v}{\partial t} \approx -c_D \frac{v}{h} + \alpha \frac{\beta_B}{h^6} + N \frac{1}{h} \frac{\partial}{\partial x} \left(\sqrt{gh} h \frac{\partial v}{\partial x} \right), \tag{A.11}$$

where

$$\alpha := 12/\sqrt{\pi} g B_r^3/\gamma^4 \geq 0, \qquad \beta_B := A^7 k \sin(\theta).$$

The wavenumber magnitude is k, the sea elevation is A, and g is gravity. B_r and γ are parameters associated with wave breaking and sea elevation, respectively. When we further assume that $\partial v/\partial t = 0$ in (A.11) we obtain the vortex force longshore balance model, (2).

Acknowledgments

We received funding from GoMRI/BP. JR and SV also received funding from NSF-DMS-1109856. We wish to thank Prof. Falk Feddersen, for discussions on current longshore models. Several suggestions by the referees improved the paper. JR also thanks the J. T. Oden Fellowship program at U. Texas, Austin, and the Aspen Center for Physics. The Aspen Center of Physics is supported, in part, by the National Science Foundation under Grant No. PHYS-1066293.

References

[1] S. J. Lentz, M. R. Fewings, The wind- and wave-driven inner shelf circulation, Annual Review of Marine Sciences 4 (2012) 317–343.

[2] Q. Chen, J. T. Kirby, R. A. Dalrymple, F. Shi, E. B. Thornton, Boussinesq modeling of longshore currents, Journal of Geophysical Research, Oceans '08 (2003) C113362.

[3] J. Choi, J. T. Kirby, S. B. Yoon, Boussinesq modeling of longshore currents in the SandyDuck experiment under directional random wave conditions, Coastal Engineering 101 (2015) 17–34.

[4] T. J. .Noyes, R. T. Guza, S. Elgar, T. H. C. Herbers, Field observations of shear waves in the surf zone, Journal of Geophysical Research, Oceans 109 (2004) C01031.

[5] T. J. .Noyes, R. T. Guza, F. Feddersen, S. Elgar, T. H. C. Herbers, Model-data comparisons of shear waves in the nearshore, Journal of Geophysical Research, Oceans 110 (2005) C05019.

[6] R. Cienfuegos, E. Barthélemy, P. Bonneton, Wave-breaking model for Boussinesq-type equations including roller effects in the mass conservation equation, Journal of Waterway, Port, Coastal, and Ocean Engineering 136 (2010) 10–26.

[7] F. Feddersen, The generation of surfzone eddies in a strong alongshore current, Journal of Physical Oceanography 44 (2014) 600–614.

[8] F. Feddersen, Breaking wave induced cross-shore tracer dispersion in the surfzone: Model results and scalings, Journal of Geophysical Research, Oceans 112 (2007) C09012. doi:10.1029/2006JC004006.

[9] S. Suanda, F. Feddersen, A self-similar scaling for cross-shelf exchange driven by transient rip currents, Geophysical Research Letters doi:10.1002/2015GL063944.
[10] O. Nwogu, Alternative form of Boussinesq equations for nearshore wave propagation, Journal of Waterways Ports and Coastal Ocean Engineering 119 (1993) 618638.
[11] A. B. Kennedy, Q. H. Chen, J. T. Kirby, R. A. Dalrymple, Boussinesq modeling of wave transformation, breaking and runup. I: One dimension, Journal of Waterways Ports and Coastal Ocean Engineering 126 (2000) 39–47.
[12] P. Lynett, Nearshore modeling using high-order Boussinesq equations, Journal of Waterways Ports and Coastal Ocean Engineering 132 (2006) 348–357.
[13] J. Allen, P. Newberger, R. Holman, Nonlinear shear instabilities of alongshore currents on plane beaches, Journal of Fluid Mechanics 310 (1996) 181–213.
[14] H. T. Ozkan-Haller, J. T. Kirby, Nonlinear evolution of shear instabilities of the longshore current: A comparison of observations and computations, Journal of Geophysical Research, Oceans 104 (1999) C11, 25953–25984.
[15] Y. Uchiyama, J. C. McWilliams, J. M. Restrepo, Wave-current interaction in nearshore shear instability analyzed with a Vortex Force formalism, Journal of Geophysical Research (2009) C06021doi:doi:10.1029/2008JC005135.
[16] C. Currin, T. Mitchell, M. Morris, D. Ylvisaker, Bayesian prediction of deterministic functions, with applications to the design and analysis of computer experiments, Journal of the American Statistical Association 86 (1991) 953?963.
[17] A. Bensoussan, J. Lions, G. Papanicolaou, Asymptotic Analysis for Periodic Structures, North-Holland, Amsterdam, 1978.
[18] J. C. McWilliams, J. M. Restrepo, E. M. Lane, An asymptotic theory for the interaction of waves and currents in coastal waters, Journal of Fluid Mechanics 511 (2004) 135–178.
[19] E. M. Lane, J. M. Restrepo, J. C. McWilliams, Wave-current interaction: A comparison of radiation-stress and vortex-force representations, Journal of Physical Oceanography 37 (2007) 1122–1141.
[20] B. Weir, Y. Uchiyama, E. Lane, J. M. Restrepo, J. C. McWilliams, A Vortex Force analysis of the interaction of rip currents and surface gravity waves, Journal of Geophysical Research 116 (2011) C050001.
[21] S. Elgar, T. H. C. Herbers, R. T. Guza, Reflection of ocean surface gravity waves from a natural beach, Journal of Physical Oceanography 24 (1994) 1503–1511.
[22] M. S. Longuet-Higgins, Longshore currents generated by obliquely incident sea waves, 1, Journal of Geophysical Research 75 (1970) 6778–6789.
[23] M. S. Longuet-Higgins, Longshore currents generated by obliquely incident sea waves, 2, Journal of Geophysical Research 75 (1970) 6790–6801.
[24] M. S. Longuet-Higgins, R. W. Stewart, Changes in form of short gravity waves on long tidal waves and tidal currents, Journal of Fluid Mechanics 8 (1960) 565–583.
[25] M. S. Longuet-Higgins, R. W. Stewart, The changes in amplitude of short gravity waves on steady non-uniform currents, Journal of Fluid Mechanics 10 (1961) 529–549.
[26] B. G. Ruessink, J. . R. Miles, F. Feddersen, R. T. Guza, S. Elgar, Modeling the alongshore current on barred beaches, Journal of Geophysical Research, Oceans 106 (2001) 22451–22463O.
[27] E. B. Thornton, R. T. Guza, Transformation of wave height distribution, Journal of Geophysical Research, C10 88 (1983) 5925–5938.
[28] J. C. Church, E. B. Thornton, Effects of breaking wave induced turbulence within a longshore current model, Coastal Engineering 20 (1993) 1–28.
[29] F. Feddersen, R. Guza, S. Elgar, T. Herbers, Velocity moments in alongshore bottom stress parameterizations, Journal of Geophysical Research, Oceans 105 (2000) 86738686.
[30] E. Lane, S. Peacock, J. M. Restrepo, A dynamic-flow carbon-cycle box model and high-latitude sensitivity, Tellus B 58 (2006) 257–278.
[31] B. S. Everitt, D. J. Hand, Finite Mixture Distributions, Chapman and Hall, Boca Raton, FL, 1981.
[32] J. C. McWilliams, J. M. Restrepo, The wave-driven ocean circulation, Journal of Physical Oceanography 29 (1999) 2523–2540.
[33] C. M. Bishop, Pattern Recognition and Machine Learning, Springer, New York, 2006.
[34] E. B. Thornton, R. T. Guza, Surf zone longshore currents and random waves: Field data and models, Journal of Physical Oceanography 16 (1986) 1165–1178.
[35] J. M. Restrepo, Wave breaking dissipation in the wave-driven ocean circulation, Journal of Physical Oceanography 37 (2007) 1749–1763.
[36] C. P. Robert, G. Casella, Monte Carlo Statistical Methods, 2nd Edition, Springer-Verlag, New York, 2004.
[37] A. Alexanderian, J. Winokur, I. Sraj, A. Srinivasan, M. Iskandarani, W. C. Thacker, O. M. Knio, Global sensitivity analysis in an ocean general circulation model: a sparse spectral projection approach, Computational Geoscience 16 (2012) 757–778. doi:10.1007/s10596-012-9286-2.
[38] C. Wunsch, The Ocean Circulation Inverse Problem, Cambridge University Press, Cambridge, UK, 1996.
[39] J. Fredsoe, R. Deigaard, Mechanics of Coastal Sediment Transport, World Scientific, 1992.
[40] M. Stive, Advances in Coastal Morphodynamics: An Overview of the G8-Coastal Morphodynamics Project; European Union, September 1992 to November 1995, Delft Hydraulics, 1995.
[41] R. L. Soulsby, Dynamics of Marine Sands, A Manual for Practical Applications, Thomas Telford, 1997.